PERGAMON

International Journal of Solids and Structures 37 (2000) 5297–5313

INTERNATIONAL JOURNAL OF SOLIDS and STRUCTURES

www.elsevier.com/locate/ijsolstr

Analysis of imperfect column buckling under intermediate velocity impact

Hong Hao*, Hee Kiat Cheong, Shijie Cui

School of Civil and Structural Engineering, Nanyang Technological University, Nanyang Avenue, Singapore 639798, Singapore

Received 23 March 1999; in revised form 20 July 1999

Abstract

This paper theoretically investigates the dynamic buckling characteristics of imperfect columns subjected to axial intermediate velocity impact loads. Based on the observations of tested columns under intermediate velocity fluid–solid impact, the dynamic buckling equation of imperfect columns is simplified and solved. A theoretical solution of the equation is derived. According to the characteristics of the theoretical solution, a dynamic buckling criterion is proposed to determine the critical buckling condition and to estimate the dynamic buckling critical load. Results obtained in the present study agree well with the experimental and numerical results. Effects of the initial imperfection, slenderness ratio of columns and dynamic load duration on dynamic buckling properties of columns under intermediate velocity impact are also discussed in the present study.

Keywords: Dynamic buckling; Imperfect columns; Intermediate velocity impact; Critical criterion; Critical load parameter

1. Introduction

Investigations of dynamic buckling of suddenly-loaded structures have received increasing attention in the past decades. Studies of dynamic buckling of suddenly-loaded columns, according to the dynamic load characteristics, can be divided into three categories, viz., high velocity impacted buckling, low velocity impacted buckling and intermediate velocity impacted buckling. On the high velocity impacted buckling of columns, the dynamic load poses a high peak value and short duration (in the microsecond magnitude). Thus, it can be simplified as an impulsive load. The dynamic buckling of columns subjected to this kind of impulsive load, therefore, is also called "pulse buckling" (Lindberg and Florence, 1987). On the other hand, for the low velocity impact load, its duration is much longer than fundamental

* Corresponding author. Tel.: +65-791-1744; fax: +65-791-0676.

0020-7683/00/$ - see front matter
PII: S0020-7683(99)00212-7

vibration periods of columns. Hence, the dynamic buckling of columns is usually considered as the buckling of columns under sudden loads with constant magnitudes and infinite duration (step load). Both high velocity and low velocity impact loads can be modeled by their magnitudes only. The effect of load duration can be neglected. Many studies have been carried out on the high velocity and low velocity impacted buckling of columns (Lindberg, 1965; Hayashi and Sano, 1972a, 1972b; Lee, 1978; Jones and dos Reis, 1980; Ari-Gur et al., 1982; Gary, 1983; Bell, 1988; Furta, 1990 and Simitses, 1990). More detailed discussions about the dynamic buckling investigations of columns can be referred to Simitses (1987), Jones (1989, 1996).

The intermediate velocity impact load has moderate duration (in the order of millisecond) so that it can neither be simplified as the impulse load nor the step load with infinite duration. Since the duration of this type of dynamic load is an important parameter that it affects significantly the dynamic buckling behaviors of columns, the load duration effect should be taken into account in the studies of suddenly-loaded columns. Some studies were performed on the dynamic buckling of columns under this type of two-parameter (magnitude and duration) intermediate velocity impact loads. Weller et al. (1989) numerically investigated the dynamic buckling of beams and plates subjected to this type of dynamic loads by using the ADINA computer code. By introducing a Dynamic Load Amplification Factor (DLF), they considered the effect of load duration and estimated the dynamic buckling critical load parameter. The results showed that both, the maximum initial imperfection and the load duration affect the dynamic buckling properties of structures. Karagiozova and Jones (1992a,b, 1995) studied the dynamic buckling phenomenon of a "spring-rigid-bar" model subjected to a rectangular pulse load and two triangular shape loads. According to the responses of the model, dynamic buckling characteristics were discussed. The effects of load duration, initial imperfection, axial inertia and hardening ratio of material on the dynamic buckling behavior of the model were also investigated.

Fluid–solid slamming is a typical intermediate velocity impact. Dynamic buckling of columns under fluid–solid slamming is frequently encountered in naval and off-shore engineering. Only a few studies on this subject, however, can be found till date, in literature. Zhang et al. (1992) experimentally tested the dynamic buckling of fixed-end columns under fluid–solid intermediate velocity impact. By using the measured axial strain, they defined critical buckling and collapse conditions of columns. Unfortunately, the estimated maximum axial strains of the columns might not correlate with the critical impact loads of the columns because the plastic collapse of a column and the corresponding impact load usually do not occur at the peak axial strain. Karagiozova and Jones (1996b) proposed a theoretical model to simulate the dynamic buckling of columns under axial slamming loads. They also compared the dynamic responses obtained from the theoretical predictions with the test results reported by Zhang et al. (1992). Recently, Cui et al. (1999a) also investigated the dynamic buckling of columns under fluid–solid slamming. Unlike those by Zhang et al. (1992) the boundary conditions of columns are hinged at both ends. The dynamic buckling critical condition was defined in terms of various fluid–solid impulse rather than the axial strains as used by Zhang et al. (1992), and the corresponding critical buckling impulse was estimated for each tested column. The dynamic buckling mechanism, buckling mode and the influences of load duration and slenderness ratios of columns on their dynamic buckling behaviors, were also discussed in the study.

This paper theoretically investigates the dynamic buckling properties of simply-supported imperfect columns subjected to intermediate velocity impact loads. A closed form solution of dynamic buckling critical load parameter, which is a function of column slenderness ratio, its maximum initial imperfection and dynamic load duration, is derived. The primary objectives of this study are to investigate the dynamic buckling mechanism of the imperfect column, to define a dynamic buckling criterion, to provide a simple and efficient method to estimate the critical load parameter and to examine the influence of imperfection and impact load duration on the dynamic buckling properties of columns.

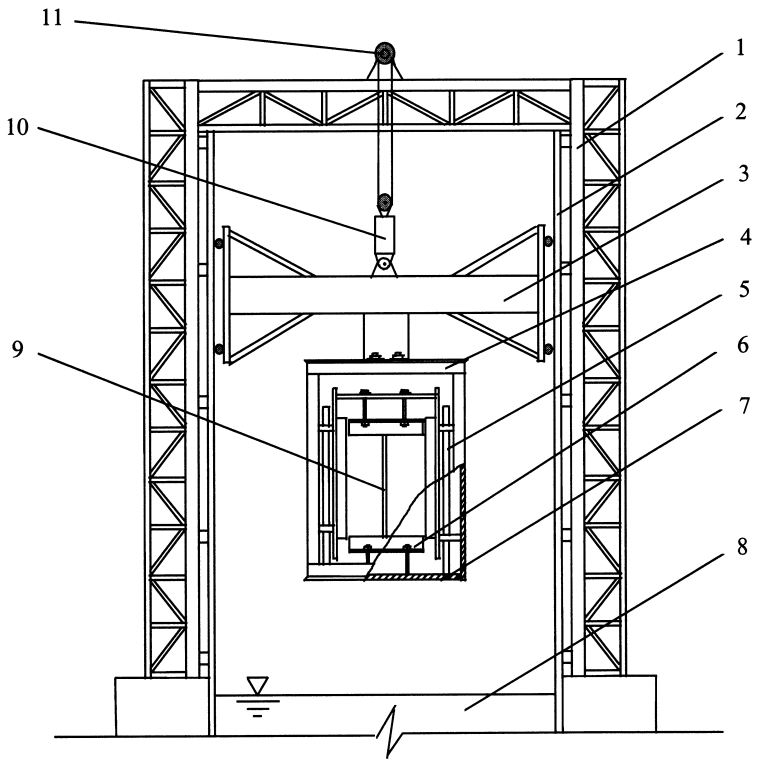

Fig. 1. Schematic view of the slamming tower and the loading device. (1) Slamming tower; (2) sliding guide; (3) slamming traverse girder; (4) loading device; (5) sliding bar; (6) simply-supported boundary; (7) bottom plate of loading device; (8) deep pool; (9) specimen; (10) electromagnetic releaser; (11) lift.

2. Brief description of experimental study

2.1. Experimental set-up and testing procedure

To study the dynamic buckling properties of columns under intermediate velocity impact, experimental tests of simply-supported columns subjected to fluid–solid slamming were performed (Cui et al., 1999a). The basic principle of the fluid–solid slamming test is to add a huge mass to the upper edge of a vertical column specimen and allow the mass and column to fall freely from a certain designed height to slam the water surface so as to induce an axial fluid–solid impact load on the column. According to this principle, a special loading device was designed, which consisted of a box frame, upper and lower fixtures (supporting boundaries) and a rigid bottom loading plate. The tests were carried out at an over-water slamming tower. The slamming tower consists of a slamming frame, a slamming traverse girder and a deep pool, as shown in Fig. 1. The traverse girder can smoothly move up (lifted by an elevator) and down along sliding guides. The loading device is suspended on the slamming traverse girder of the tower (Fig. 1). The upper end of specimen is connected to the upper supporting boundary of the loading device, and the lower end to the lower boundary, and then to a bottom plate which is separated from the loading device and can move up and down freely together with the smooth sliding bars.

To capture the response of the loaded columns, strain gauges were stuck symmetrically on both sides

Table 1
Theoretical and experimental dynamic buckling load parameters for 12 columns

No.	L (mm)	b (mm)	h (mm)	λ	δ_{0max} (mm)	t_0 (s)	α_E	α_{cr} Eq. (40)	Error (%)
1	500	14.74	8.64	200.47	0.20	0.021	1.975	1.978	0.25
2	500	14.53	8.70	199.09	0.20	0.021	1.928	1.985	2.96
3	500	14.62	10.65	162.63	0.21	0.018	2.398	2.423	1.04
4	500	14.45	10.68	162.18	0.10	0.018	2.345	2.477	5.63
5	500	14.64	12.42	139.46	0.66	0.0175	2.463	2.534	2.88
6	500	14.88	12.20	141.97	0.34	0.0175	2.553	2.632	3.09
7	450	14.84	8.86	175.94	0.18	0.0185	2.044	2.160	5.68
8	450	14.77	8.84	176.34	0.17	0.0185	2.142	2.151	0.42
9	450	14.78	10.80	144.34	0.26	0.0178	2.364	2.438	3.13
10	450	14.49	10.74	145.14	0.26	0.0178	2.412	2.429	0.71
11	450	14.48	12.15	128.30	0.76	0.0165	2.485	2.547	2.49
12	450	14.51	12.28	126.94	0.15	0.0165	2.661	2.835	6.54
								mean	2.90

at several measuring points along the column. In each test, the whole system, including the loading device and transverse girder, is lifted up to a certain height and then released, to allow a free fall. When the loading device slams the water, the speed of the bottom plate will slow down due to its relatively large contact area with water surface, the other parts of the loading device will, however, sink into water at a much faster speed. Thus, a fluid–solid slamming load is induced and applied to the column specimen as an intermediate velocity axial impact load. The dynamic strain signals measured by strain gauges are amplified first and then recorded. At the same time, the impulse S produced by slamming is computed from the measured mass of the whole moving system and the velocity when the system is about to slam the water surface.

Dimensions and parameters of 12 tested columns are shown in Table 1, in which L, b, h, λ and δ_{0max} are the length, width, thickness, the slenderness ratio and the maximum initial imperfection of the columns. The elastic modulus of column material was obtained from tensile tests as $E = 2.11 \times 10^5$ MPa, and the stress wave velocity $c = 5190$ m/s. These columns will be used to verify the theoretical solution derived in this study. More detailed description of the test can be referred to Cui et al. (1999a).

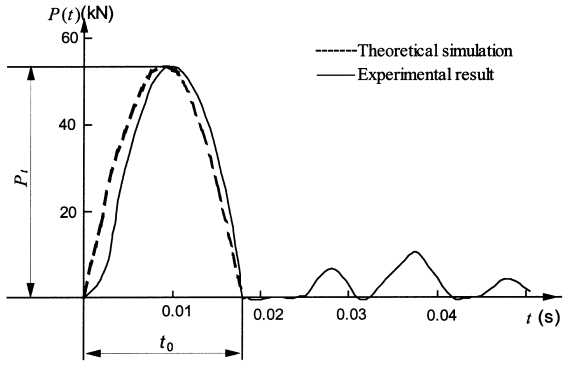

Fig. 2. A typical axial slamming load time history.

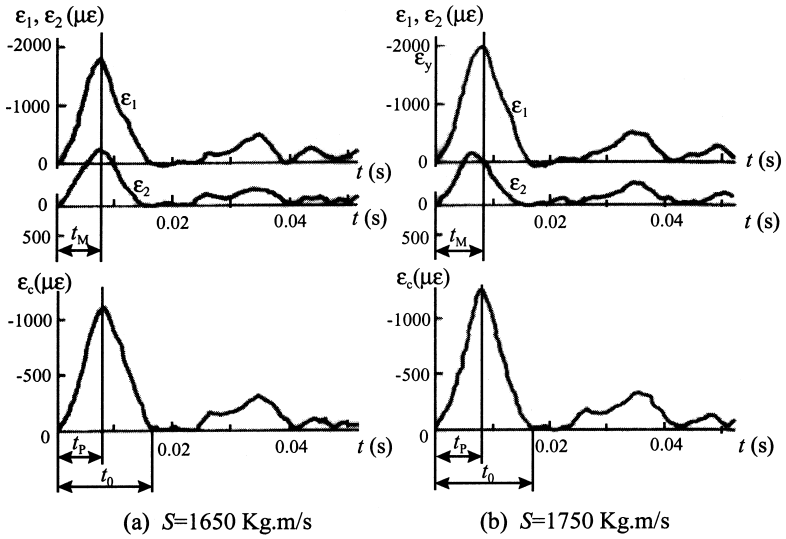

Fig. 3. Dynamic responses of a column under impulses.

2.2. Some observations from the experiments

To begin with the theoretical study of imperfect columns under intermediate velocity impact, some observations from the fluid–solid slammed columns are introduced first.

By slamming each column with different slamming heights in the experiments, a series of slamming loads and dynamic responses of columns under different slamming impulses were recorded. Fig. 2 shows a typical axial slamming load time history, in which the first waveform is produced by slamming the specimen to water surface, and the following smaller waveforms after t_0 are secondary waves induced from oscillation of the loading device in water after slamming. It is obvious that the secondary waveforms are far smaller than the primary one due to slamming, implying the effects of these secondary waves can be neglected. Therefore, the fluid–solid axial impact load could be approximated by a half-sine shape, that is

$$P(t) = \begin{cases} P_t \sin \theta t & 0 \le t \le t_0 \\ 0 & t > t_0 \end{cases} \tag{1}$$

in which $\theta = \pi/t_0$; P_t and t_0 are peak value and duration of the dynamic load, respectively. Using Eq. (1) with $P_t = 53.5$ kN and duration $t_0 = 0.018$ s, the approximated impact load time history is also estimated and plotted in Fig. 2. As can be seen, the half-sine function can indeed approximate the fluid–solid axial impact load.

It can be observed from the experimental tests that the duration of fluid–solid slamming load depends on the slenderness ratio of columns. The larger the slenderness ratio, the longer the dynamic load duration. For the columns with the same slenderness ratios, the duration is approximately the same. For the 12 tested columns with slenderness ratios of about 127–200, the duration is between 0.0165 and 0.021 s, which are also shown in Table 1.

Fig. 3 shows the dynamic responses of a column under impulses $S = 1650$ and 1750 kg m/s, in which ε_c is the axial compressive strain at the slamming end of the column, ε_1 and ε_2 are the compressive-

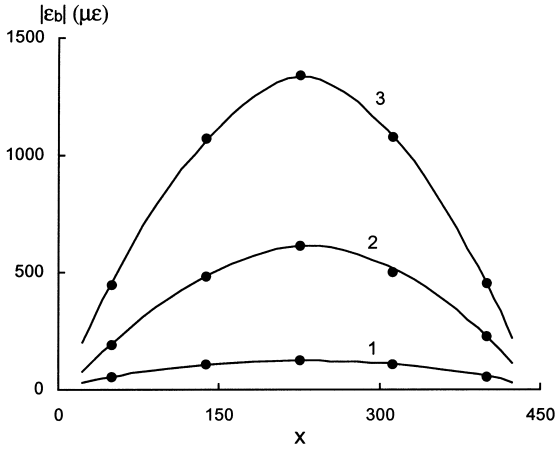

Fig. 4. Distribution of ε_b along the length of column. (1) $S = 1213$ kg m/s; (2) $S = 1697$ kg m/s; (3) $S = 1880$ kg m/s.

bending resultant strains on both sides at the middle height of the column, respectively. It can be easily found that, for the column subjected to an intermediate velocity fluid–solid slamming, the peak responses always occur during the load duration at about $t_0/2$. This observation agrees with that obtained by Zhang et al. (1992) and Karagiozova and Jones (1992b) for a column under a triangular shape dynamic load, and is different from that of high velocity impacted columns in which the flexural deformation of columns usually develops greatly after the loading is released because the load duration is very short.

Another characteristic of the dynamic responses of column is that its flexural deformation strongly depends on the axial slamming load (impulse). When the axial slamming load is small, it was observed that the transverse flexural vibration of column is insignificant such that the primary response is caused by its axial compressive vibration. With the increase of slamming load, the bending vibration of the column becomes more and more pronounced. As the slamming load increases to a certain level, the response characteristics of columns are qualitatively changed from those dominated by axial compressive vibration to those dominated by transverse flexural vibration. The condition that the dominant vibration characteristic changes from axial compressive vibration to flexural vibration was defined as the dynamic buckling critical condition, and from that, the dynamic buckling critical load parameter was determined for each column. The dynamic buckling critical load parameter (α_E) from the experimental tests are also listed in Table 1.

Fig. 4 shows the distribution of bending strain along the length of a column under different impulses. It is clear that the lateral responses of column under different slamming loads always have half-sine waveforms. This indicates that the dynamic buckling mode of simply-supported columns under fluid–solid slamming is governed by the fundamental vibration mode of the column. This observation is also different from that of columns under solid–solid impact. For the later case, higher buckling modes are usually induced due to the high velocity impact (Lindberg and Florence, 1987; Karagiozova and Jones, 1996a). More detailed information and discussions of the experimental tests of the columns under fluid–solid slamming can be referred to the previous paper by Cui et al. (1999a).

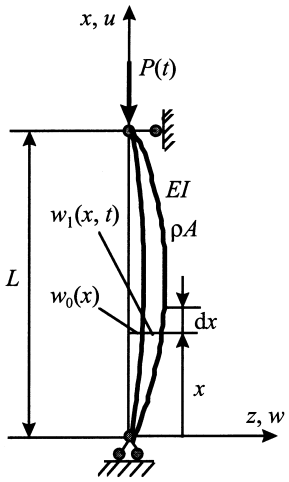

Fig. 5. Column under intermediate velocity impact.

3. Dynamic buckling equation and its solution

3.1. Dynamic buckling equation

Consider an imperfect column subjected to an intermediate velocity impact load, $P(t)$, as shown in Fig. 5. The column has length L, cross-section area A, flexural stiffness EI and the mass density per unit length ρ. The imperfection of the column is considered as an initial transverse bending deformation $w_0(x)$. The transverse displacement response induced by the dynamic load is a function of position x and time t and denoted by $w_1(x, t)$. The axial impact load is assumed to have a half-sine shape as shown in Eq. (1). As indicated in the above section, for the fluid–solid slammed columns with slenderness ratios of about 127–200 as listed in Table 1, the duration t_0 is between 0.0165 and 0.021 s. During that duration, axial waves will propagate along the column back and forth about 173–228 times. This indicates that the effect of axial inertia is insignificant for the present columns. Thus, by ignoring the axial inertia, the dynamic equilibrium equation of the column can be obtained as follows:

$$\begin{cases} EI\dfrac{\partial^4 w_1}{\partial x^4} + P(t)\dfrac{\partial^2 w_1}{\partial x^2} + \rho A\dfrac{\partial^2 w_1}{\partial t^2} = -P(t)\dfrac{\partial^2 w_0}{\partial x^2} \\ w_1(x, 0) = f(x) \\ \dfrac{\partial w_1}{\partial t}(x, 0) = g(x) \end{cases} \tag{2}$$

where $f(x)$ and $g(x)$ are the initial displacement and initial velocity functions of the column. It should be noted that the effect of damping is not considered in this study.

By introducing the following parameters

$$\begin{cases} y = \dfrac{w_1}{r}, & \xi = kx, & \tau = \dfrac{s^2 c}{r} t = \dfrac{t}{\eta}, \\ r^2 = \dfrac{I}{A}, & k^2 = \dfrac{P_{\mathrm{E}}}{EI}, & c^2 = \dfrac{E}{\rho}, \qquad \tau_0 = \dfrac{t_0}{\eta}, \\ s^2 = r^2 k^2, & \alpha = \dfrac{P_t}{P_{\mathrm{E}}}, & l = \dfrac{sL}{r} \end{cases} \tag{3}$$

in which P_{E} is the Euler static critical load of column, c is the stress wave velocity of column material, and α is defined as a non-dimensional dynamic load parameter. The Eq. (2) can be rewritten in a dimensionless form as

$$\begin{cases} y'''' + \alpha \sin \theta\eta\tau y'' + \ddot{y} = -\alpha \sin \theta\eta\tau y_0'' \\ y(\xi, 0) = f(\xi) \\ \dot{y}(\xi, 0) = g(\xi) \end{cases} \tag{4}$$

in which the prime indicates differentiation with respect to the axial coordinate x of the column and the dot the differentiation with respect to time t.

It should be noted that the coefficient of y'' is not a constant, but varies with two parameters, namely the peak load parameter α and the time τ. To get the solution of this equation, the response $y(\xi, \tau)$ and the initial bending deformation $y_0(\xi, 0)$ of the column are decomposed into its modal coordinates as

$$\begin{cases} y(\xi, \tau) = \displaystyle\sum_{n=1}^{\infty} g_n(\tau)\phi_n(\xi) \\ y_0(\xi, 0) = \displaystyle\sum_{n=1}^{\infty} \bar{\delta}_n \phi_n(\xi) \end{cases} \tag{5}$$

where $\phi_n(\xi)$ is the nth vibration mode shape, $g_n(\tau)$ is the corresponding nth modal coordinate and $\bar{\delta}_n = \bar{\delta}_{n\,\max}/r = 2\sqrt{3}\bar{\delta}_{n\,\max}/h = 2\sqrt{3}\bar{\delta}_n^*$ is the corresponding nth modal dimensionless maximum imperfection. Substituting Eq. (5) into Eq. (4), and using orthogonality conditions of the mode shape, the dynamic buckling equation of the column can be derived as

$$\begin{cases} \ddot{g}_n(\tau) + \dfrac{n^4\pi^4}{l^4} q(\tau) g_n(\tau) = \dfrac{n^4\pi^4}{l^4} \bar{\delta}_n \alpha \sin \theta\eta\tau \\ g_n(0) = \bar{f}_n \qquad\qquad 0 \le \tau \le \dfrac{t_0}{\eta} \\ \dot{g}_n(0) = \bar{g}_n \end{cases} \tag{6}$$

in which $q(\tau) = 1 - \alpha_n \sin \theta\eta\tau$; and $\bar{f}_n = \frac{2}{l}\int_0^l f(\xi)\phi_n(\xi)\,\mathrm{d}\xi$ and $\bar{g}_n = \frac{2}{l}\int_0^l g(\xi)\phi_n(\xi)\,\mathrm{d}\xi$ are generalized initial displacement and velocity corresponding to the nth mode. It should be noted that in most cases the initial displacement and initial velocity will be zero. Without losing generality, however, their general forms are given in the present derivation. Since columns observed in the tests all buckled in their first mode, the subscript "n" is dropped hereafter in the derivation.

3.2. Solution of the dynamic buckling equation

In order to obtain the solution of Eq. (6), two dimensionless time parameters are introduced herein

$$\mu_1 = \frac{1}{\theta\eta}\arcsin\frac{1}{\alpha} \quad \text{and} \quad \mu_2 = \frac{\pi}{\theta\eta} - \mu_1 \tag{7}$$

Inspecting the properties of function $q(\tau)$, it can be found that: (i) $q(\tau) > 0$, when $\tau < \mu_1$ and $\tau > \mu_2$; (ii) $q(\tau) < 0$, when $\mu_1 < \tau < \mu_2$; and (iii) $q(\tau) = 0$, when $\tau = \mu_1 = \mu_2$. From these properties of function $q(\tau)$, it is obvious that the solution of Eq. (6) is oscillatory when $\tau < \mu_1$ and $\tau > \mu_2$, while it is exponential when $\mu_1 < \tau < \mu_2$. This indicates that buckling of the column may only occur in the duration between μ_1 and μ_2. Therefore, the following derivation is focused on getting the solution of Eq. (6) in the duration of μ_1 and μ_2. The solution of the equation when $\tau < \mu_1$, however, is also needed to determine the integral constants in terms of the initial conditions.

Eq. (6) is a typical turning point problem. At time $\tau = \mu_1$, $q(\tau)$ is singular and the equation has a turning point at which the property of solution is qualitatively changed from oscillatory to exponential. This kind of turning point problem can be solved by the powerful Langer transformation method (Nayfeh, 1973).

Using the transformation

$$z = \lambda^{1/2}\phi(\tau), \qquad v = \dot{\phi}^{1/2}\left[g(\tau) + \bar{\delta}\right] \quad \text{and} \quad \dot{\phi}^2\phi = q(\tau) \tag{8}$$

and dropping the subscript n, Eq. (6) can be rewritten as

$$\frac{\mathrm{d}^2 v}{\mathrm{d}z^2} + \frac{1}{K^2}zv = \frac{\pi^4}{l^4\lambda}\sqrt{\alpha\theta\eta}\bar{\delta} + \delta_1 v \tag{9}$$

in which

$$K^2 = \frac{l^4\lambda^{3/2}}{\pi^4} + \frac{17(\theta\eta\tau_0)^4 l^6\left(4\sqrt{6} - \bar{\delta}\right)}{(1-\alpha)\tau_0\lambda^{1/2}\pi^2\left(2\sqrt{3} + l\bar{\delta}\right)} \tag{10}$$

$$\delta_1 = -\frac{\pi^6 l^{-2}\bar{m}\phi}{l^2(\theta\eta\tau_0)^2\bar{m} + \tau_0 l^2\lambda^2\left(2\sqrt{3} + l\bar{\delta}\right)q(\tau)} + \frac{1}{4\lambda}\phi^{-1}\dot{\phi}^{-4}\alpha\theta^2\sin\theta\eta\tau + \frac{5}{16\lambda}\phi^{-2}\sin^2\theta\eta\tau \tag{11}$$

$$\bar{m} = 34\sqrt{3}(\theta\eta\tau_0)^2\pi^2 l^2\lambda^{-1}\left(2\sqrt{2} - \bar{\delta}^*\right)\left(\dot{\phi}^3 + 2\phi\dot{\phi}\ddot{\phi}\right)\mu_1 \tag{12}$$

If $1/K^2$ is much larger than δ_1, that is

$$\frac{1}{K^2} \geq \varepsilon^{-1}|\delta_1|_{\max} \quad \text{or} \quad K^2 \leq \varepsilon|1/\delta_1|_{\max} \tag{13}$$

where δ_1 is given in Eq. (11), and ε is a small positive number, Eq. (9) can be approximated as

$$\frac{\mathrm{d}^2 v}{\mathrm{d}z^2} + \frac{1}{K^2}zv = \frac{\pi^4}{l^4\lambda}\sqrt{\alpha\theta\eta}\bar{\delta} \tag{14}$$

The homogeneous equation (14) can be transformed to a Bessel equation of order one third. Thus, the homogeneous solution of Eq. (14) can be obtained as (Cui et al., 1999b)

$$\bar{v} = C_1 Ai(-K^{-2/3}z) + C_2 Bi(-K^{-2/3}z) \tag{15}$$

in which C_1 and C_2 are constants to be determined, $Ai(z)$ and $Bi(z)$ are the Airy functions of the first

and second kind, respectively. They are

$$Ai(-z) = \frac{1}{\sqrt{\pi}} z^{-1/4} \sin\left(\eta + \frac{\pi}{4}\right),$$

$$Bi(-z) = \frac{1}{\sqrt{\pi}} z^{-1/4} \cos\left(\eta + \frac{\pi}{4}\right), \quad z < 0 \tag{16}$$

and

$$Ai(z) = \frac{1}{2\sqrt{\pi}} z^{-1/4} \exp(-\eta)$$

$$Bi(z) = \frac{1}{\sqrt{\pi}} z^{-1/4} \exp(\eta), \quad z > 0 \tag{17}$$

in which $\eta = \frac{2}{3} z^{3/2}$. To obtain the particular solution of Eq. (14), φ_1 and φ_2 are introduced as

$$\varphi_1 = Ai(-K^{-2/3} z) \qquad \varphi_2 = Bi(-K^{-2/3} z) \tag{18}$$

and let the particular solution be

$$v^* = E_1(z)\varphi_1 + E_2(z)\varphi_2 \tag{19}$$

by substituting Eq. (19) into (14), it has

$$\begin{cases} E_1'(z)\varphi_1 + E_2'(z)\varphi_2 = 0 \\ E_1'(z)\varphi_1' + E_2'(z)\varphi_2' = \bar{\delta}_\alpha \end{cases} \tag{20}$$

in which $\bar{\delta}_\alpha = (\pi^4/l^4\lambda)\sqrt{\alpha\theta\eta}\bar{\delta}$. $E_1(z)$ and $E_2(z)$ can be obtained from Eq. (20) as

$$E_1(z) = -\bar{\delta}_\alpha \int \frac{\varphi_2}{u}\, \mathrm{d}z \qquad E_2(z) = \bar{\delta}_\alpha \int \frac{\varphi_1}{u}\, \mathrm{d}z \tag{21}$$

where

$$u = \varphi_1\varphi_2' - \varphi_2\varphi_1' \tag{22}$$

Thus, the approximate solution of Eq. (6) can be expressed as follows:

For $\tau < \mu_1$,

$$g(\tau) = \frac{K_1}{\sqrt[4]{q(\tau)}}(C_1 \sin\psi + C_2 \cos\psi) + \beta(\tau)\bar{\delta} \tag{23}$$

and for $\mu_1 < \tau < \mu_2$,

$$g(\tau) = \frac{K_1}{\sqrt[4]{-q(\tau)}}\left(\frac{C_1}{2} e^{-\phi} + C_2 e^{\phi}\right) + \gamma(\tau)\bar{\delta} \tag{24}$$

in which

$$\beta(\tau) = \frac{K_1\pi^4}{l^4\lambda}\frac{\sqrt{\alpha\theta\eta}}{\sqrt[4]{q(\tau)}}\cos\psi\left[\int_\tau^{\mu_1}\frac{\cos\psi}{\sqrt[4]{q(u)}}\,\mathrm{d}u - \tan\psi\int_\tau^{\mu_1}\frac{\sin\psi}{\sqrt[4]{q(u)}}\,\mathrm{d}u\right] \tag{25}$$

$$\gamma(\tau) = \frac{K_1\pi^4}{2l^4\lambda}\frac{\sqrt{\alpha\theta\eta}}{\sqrt[4]{-q(\tau)}}\mathrm{e}^{\phi}\left[\int_{\mu_1}^{\tau}\frac{\mathrm{e}^{\phi}}{\sqrt[4]{-q(u)}}\,\mathrm{d}u - \mathrm{e}^{-2\phi}\int_{\mu_1}^{\tau}\frac{\mathrm{e}^{-\phi}}{\sqrt[4]{-q(u)}}\,\mathrm{d}u\right] \tag{26}$$

$$\psi = \frac{1}{K}\int_\tau^{\mu_1}\sqrt{q(u)}\,\mathrm{d}u + \frac{\pi}{4}$$

$$\phi = \frac{1}{K}\int_{\mu_1}^{\tau}\sqrt{-q(u)}\,\mathrm{d}u$$

$$K_1 = \frac{\lambda^{5/12}r^{1/6}}{\pi^{5/6}c^{1/6}} \tag{27}$$

3.3. Validity of the approximate approach

The above solution to the dynamic buckling equation (6) are obtained based on the assumption that $1/K^2 \gg \delta$ as indicated in Section 3.2, the validity of the solution depends on the correctness of this assumption. By using the transformation (8), expressions of ϕ, $\dot{\phi}$ and $\ddot{\phi}$ can be obtained. Then substituting these expressions into Eq. (11), it can be obtained from Eq. (13) that if and only if

$$\frac{\pi^{-23/3}\left(4-\sqrt{2}\bar{\delta}^*\right)}{\tau_0^{1/3}\lambda^{3/2}\left(1+l\bar{\delta}^*\right)} \le 2\sqrt{2}\left(\frac{s^2c}{r}\right)^{2/3} \tag{28}$$

the above assumption is valid. This is the condition for the validity of above solution of dynamic buckling equation. It is easy to check that all the 12 tested columns listed in Table 1 satisfy the validity condition.

4. Dynamic response and buckling condition of columns

4.1. Response of an intermediate velocity impacted column

As indicated in Section 3.2, the dynamic buckling mode of a simply-supported column under intermediate velocity impact loads is governed by the fundamental mode of its transverse bending vibration. Based on this observation, the transverse motion of the column can be approximately expressed by its first modal response as

$$y(\xi,\tau) = g_1(\tau)\sin\frac{\pi\xi}{l} \tag{29}$$

From Eq. (23) and (24), the response of the column can be given as

$$y(\xi,\tau)=\left[\frac{K_1}{\sqrt[4]{q(\tau)}}(C_1\sin\psi+C_2\cos\psi)+\beta(\tau)\bar{\delta}\right]\sin\frac{\pi\xi}{l}\quad\text{for }\tau<\mu_1 \tag{30}$$

and

$$y(\xi,\tau)=\left[\frac{K_1}{\sqrt[4]{-q(\tau)}}\left(\frac{C_1}{2}\mathrm{e}^{-\phi}+C_2\mathrm{e}^{\phi}\right)+\gamma(\tau)\bar{\delta}\right]\sin\frac{\pi\xi}{l}\quad\text{for }\mu_1<\tau<\mu_2, \tag{31}$$

in which C_1 and C_2 are constants and can be determined from the initial conditions:

$$g(0)=\bar{f}_1,\qquad \dot{g}(0)=\bar{g}_1 \tag{32}$$

From Eq. (30) and (31), it has

$$\begin{cases} K_1\left[C_1\Psi_1(0)+C_2\Psi_2(0)\right]+\beta(0)\bar{\delta}=\bar{f}_1 \\ K_1\left[C_1\dot{\Psi}_1(0)+C_2\dot{\Psi}_2(0)\right]+\dot{\beta}(0)\bar{\delta}=\bar{g}_1 \end{cases} \tag{33}$$

where

$$\begin{cases} \Psi_1(0)=\sin\psi_0 \\ \Psi_2(0)=\cos\psi_0 \\ \dot{\Psi}_1(0)=\dfrac{1}{4}\alpha\theta\eta\Psi_1(0)+\dot{\psi}_0\Psi_2(0) \\ \dot{\Psi}_2(0)=\dfrac{1}{4}\alpha\theta\eta\Psi_2(0)-\dot{\psi}_0\Psi_1(0) \end{cases} \tag{34}$$

Solving Eq. (33), the integration constants C_1 and C_2 are obtained, and then from Eqs. (30) and (31), the response of the intermediate velocity impacted column can be obtained as

$$y(\xi,\tau)=g_1(\tau)\sin\frac{\pi\xi}{l}=\left[A_1(\tau)\bar{f}_1+B_1(\tau)\bar{g}_1+D_1(\tau)\bar{\delta}\right]\sin\frac{\pi\xi}{l} \tag{35}$$

in which

$$\begin{cases} A_1(\tau)=\dfrac{r\lambda^{5/2}}{\pi^2 c}\left[\dot{\Psi}_2(0)X_1(\tau)-\dot{\Psi}_1(0)X_2(\tau)\right] \\ B_1(\tau)=\dfrac{r\lambda^{5/2}}{\pi^2 c}\left[\Psi_1(0)X_2(\tau)-\Psi_2(0)X_1(\tau)\right] \\ D_1(\tau)=\Re(\tau)+\left[A_1(\tau)\beta(0)+B_1(\tau)\dot{\beta}(0)\right] \end{cases} \tag{36}$$

where, for $\tau<\mu_1$,

$$X_1(\tau)=q^{-1/4}(\tau)\sin\left[\frac{1}{K}\int_\tau^{\mu_1}\sqrt{q(u)}\,\mathrm{d}u+\frac{\pi}{4}\right]$$

$$X_2(\tau)=q^{-1/4}(\tau)\cos\left[\frac{1}{K}\int_\tau^{\mu_1}\sqrt{q(u)}\,\mathrm{d}u+\frac{\pi}{4}\right]$$

$$\Re(\tau) = \beta(\tau) \tag{37}$$

and for $\mu_1 < \tau < \mu_2$,

$$X_1(\tau) = \frac{1}{2}\left[-q(\tau)\right]^{-1/4}\exp\left[-\frac{1}{K}\int_{\mu_1}^{\tau}\sqrt{-q(u)}\,\mathrm{d}u\right]$$

$$X_2(\tau) = \left[-q(\tau)\right]^{-1/4}\exp\left[\frac{1}{K}\int_{\mu_1}^{\tau}\sqrt{-q(u)}\,\mathrm{d}u\right]$$

$$\Re(\tau) = \gamma(\tau) \tag{38}$$

in which $\beta(\tau)$ and $\gamma(\tau)$ are given in Eqs. (25) and (26).

4.2. Dynamic buckling criterion

By inspecting Eq. (35), it is clear that, for the column under intermediate velocity impact, the response of the column is caused by amplifying the initial displacement, initial velocity and initial imperfection of the column. $A_1(\tau)$, $B_1(\tau)$ and $D_1(\tau)$ are the corresponding amplification functions. In the expression of $D_1(\tau)$ as shown in Eq. (36), the first term is induced by the imperfection itself, and the second one is the coupled term of the imperfection and the initial disturbances. Thus, the dynamic response of the column can be regarded as the amplifications of the initial displacement, initial velocity or the imperfection of the column. When the dynamic load is small, the column vibrates laterally about the near static equilibrium position. If the dynamic load is large enough, the column may experience a very large vibration, or a divergent type of motion, which results in dynamic buckling. Hence, the dynamic buckling of column is a 'divergent type of buckling' (Simitses, 1990). Dynamic buckling of a column is considered to take place if the initial disturbance and/or the initial imperfection are amplified by the dynamic load to such a level that the response increases infinitely.

From Eqs. (36), (38) and (26), it can be found that the amplification functions $A_1(\tau)$, $B_1(\tau)$ or $D_1(\tau)$ will increase infinitely if and only if

$$\frac{1}{K}\int_{\mu_1}^{\tau}\sqrt{-q(u)}\,\mathrm{d}u \to \infty \tag{39}$$

Because the function $q(\tau)$ is negative in the duration between μ_1 and μ_2, the definite integral in expression (39) is a positive constant. Thus, the condition (39) becomes $K \to 0$. From Eq. (10), and noted that $\theta = \pi/t_0$ and $\tau_0 = t_0/\eta$, it can be obtained that

$$\alpha_{\mathrm{cr}} = 1 + \frac{17\pi^6 l^2\left(4\sqrt{6} - \bar{\delta}\right)}{\tau_0\lambda^2\left(2\sqrt{3} + l\bar{\delta}\right)} \tag{40}$$

This is the formula to be used to estimate the dynamic buckling critical load parameter of the column.

As a special case, when the column is straight, namely the initial imperfection is zero, Eq. (40) becomes

$$\alpha_{\mathrm{cr}} = 1 + \frac{34\sqrt{2}\pi^6 l^2}{\tau_0\lambda^2} \tag{41}$$

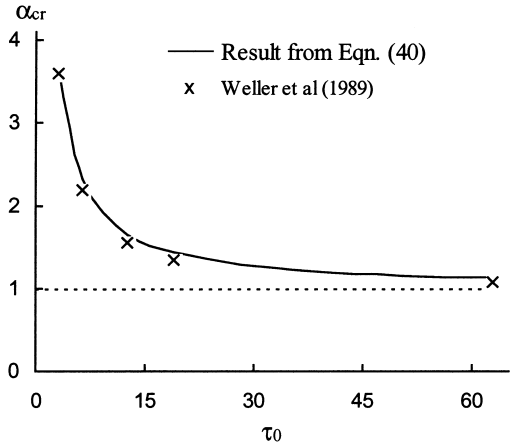

Fig. 6. Comparing with the numerical results ($\bar{\delta}^* = w_0/h = 0.10$).

This is the formula to estimate the dynamic buckling critical load parameter of straight column. This is identical to that obtained by the analysis of dynamic buckling of straight columns under intermediate velocity impact (Cui et al., 1999b).

5. Results and discussions

5.1. Comparing with the experimental and numerical results

Using the actual constants of the 12 tested column specimens and the t_0 value measured from each

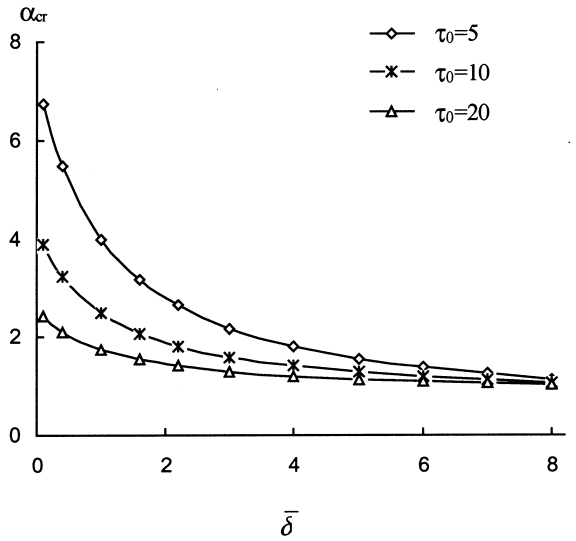

Fig. 7. Effect of initial imperfection of column.

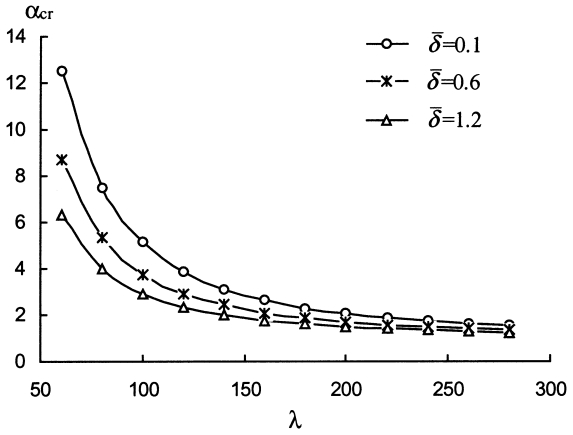

Fig. 8. Relationship between α_{cr} and λ.

test as listed in Table 1, the dynamic buckling critical load parameter α_{cr} for each column is estimated by using Eq. (40). The estimated value of α_{cr} is given in the table. It can be seen that the theoretical results agree well with the experimental results. The errors are about 0.25–6.54% for the 12 tested columns with an average error of 2.9%. The error between the theoretical and the experimental results might be attributed to the facts that: (1) theoretical impact load is not exactly the same as the actual impact load as shown in Fig. 2; and (2) small loading eccentricity is inevitable for each column in the test, but no loading eccentricity is considered in the theoretical study. This also explains why the theoretical α_{cr} is always larger than the experimental one.

Results obtained in this study are also compared with the numerical results presented by Weller et al. (1989). Using ADINA computer code, they investigated the dynamic buckling of columns and plates under axial impact. The numerical results obtained by them and the theoretical results estimated by using Eq. (40) for a column with $\bar{\delta}^* = w_0/h = 0.10$ are shown in Fig. 6. It can be seen that the theoretical results obtained in the present study also agree well with the numerical results.

5.2. Effect of initial imperfection of columns

To investigate the effect of initial imperfection of column on its dynamic buckling critical load, Fig. 7 shows the variation of dimensionless critical buckling load versus imperfection of column with $\tau_0 = 5$, 10 and 20, respectively. It is obvious from the figure that the critical buckling load of column is very sensitive to its initial imperfection, especially when the loading duration is short and initial imperfection is small. In the cases when the initial imperfection is small, i.e. $\bar{\delta} < 4$, the effect of imperfection on the dynamic buckling behaviors of column is very significant. The critical buckling load of column decreases rapidly as the imperfection increases. When $\bar{\delta} \geq 4$, however, the relationship between α_{cr} and $\bar{\delta}$ is basically linear, and the effect of imperfection is not very pronounced. Moreover, it can also be found from the figure that the load duration will influence the sensitiveness of imperfection. When the duration is large (i.e. $\tau_0 \geq 10$), the effect of column imperfection on its buckling load is less significant. As the imperfection decreases, the dynamic buckling load of column increases but this increase is not outstanding. When the load duration is small (i.e. $\tau_0 \leq 5$), the column buckling load increases sharply as the imperfection decreases. These observations indicate that the load duration strongly affects either the dynamic buckling load or the sensitiveness of the column imperfection. The above observations are the

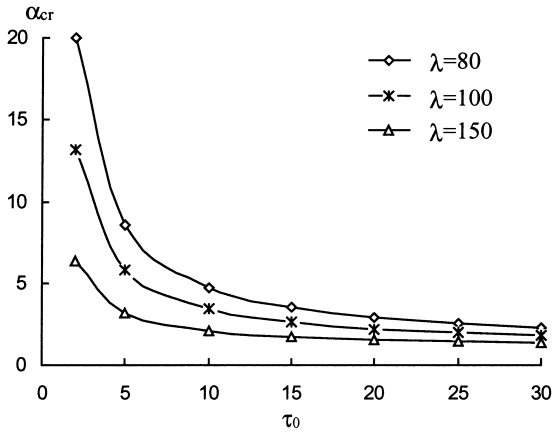

Fig. 9. Critical load parameter versus load duration.

same with those obtained by Karagiozova and Jones (1992b) in the study of a "spring-rigid-bar" model subjected to a rectangular and two triangular pulse loads.

5.3. Effect of slenderness ratio and duration

Fig. 8 shows the variation of dynamic buckling critical load parameter α_{cr} with respect to slenderness ratio λ for columns with imperfection $\bar{\delta} = 0.1$, 0.6 and 1.2, respectively. It can be seen from the figure that, as expected, the smaller the slenderness ratio of a column, the higher the critical load parameter. The critical load parameter decreases exponentially with the increase of λ. When λ is large, its effect on the column dynamic buckling critical load parameter is less pronounced, especially when the imperfection of column is large. This observation indicates that, for columns with small slenderness ratios, reducing slenderness ratio is very effective in preventing the dynamic buckling of columns.

To inspect the influence of dynamic load duration on the dynamic buckling properties of columns, Fig. 9 displays the critical load parameter α_{cr} vs. the impact load duration τ_0 for columns with different slenderness ratios. It can be found that the critical load parameter α_{cr} increases significantly as τ_0 decreases. When $\tau_0 \leq 5$, the case can be considered as a high velocity impact problem (load duration is in an order of microsecond), the α_{cr} increases sharply with the decrease of τ_0. As τ_0 tends to zero, the α_{cr} approaches infinity theoretically. On the other hand, when τ_0 approaches infinity, the case can be considered as a static loading problem, the α_{cr} tends to unity. This indicates that, for columns under intermediate velocity impact, the dynamic buckling critical load is always larger than its static buckling load.

6. Conclusions

Theoretical study of dynamic buckling of imperfect columns under axial intermediate velocity impact loads has been carried out. A theoretical solution of the dynamic buckling equation was obtained. A dynamic buckling criterion was defined and a simple formula for estimating the dynamic buckling critical load parameter as a function of column slenderness ratio, initial imperfection and impact load duration has been derived. The validity of the formula has been proven by comparing the theoretical results with both experimental and numerical results.

It was also found that a column under a two-parameter intermediate velocity impact load buckles because the dynamic load amplifies its initial imperfection. The initial imperfection, load duration and slenderness ratio of column strongly affect the dynamic buckling properties of columns. The smaller the initial imperfection of column, the higher the dynamic buckling critical load. For columns with prescribed imperfection and load duration, the dynamic buckling critical load will increase rapidly as the slenderness ratio of column decreases. Thus, reducing slenderness ratio is very effective in preventing dynamic buckling of columns.

Load duration not only strongly affects the column critical buckling load, but also the sensitivity of the initial imperfection. A column subjected to a short duration dynamic load can sustain a higher buckling load. The larger is the impact load duration, the less significant the column imperfection will be on the dynamic buckling critical load parameter.

References

Ari-Gur, J., Weller, T., Singer, J., 1982. Experimental and theoretical studies of columns under axial impact. Int. J. Solids Struct 18 (7), 619–641.

Bell, J.F., 1988. Dynamic buckling of rods at large plastic strain. Acta Mechanica 74 (1-4), 51–67.

Cui, S., Cheong, H.K., Hao, H., 1999a. Experimental study on dynamic buckling of simply-supported columns under axial slamming. Journal of Engineering Mechanics, ASCE 125 (5), 513–520.

Cui, S., Hao, H., Cheong, H.K., 1999b. Theoretical study of dynamic buckling of straight columns subjected to intermediate velocity impact loads. International Journal of Structural Engineering and Mechanics, Submitted.

Furta, S.D., 1990. Dynamic stability of an elastic column. Applied Mathematics and Mechanics 54 (6), 769–776.

Gary, G., 1983. Dynamic buckling of an elastoplastic column. Int. J. Impact Eng 1 (4), 357–375.

Hayashi, T., Sano, Y., 1972a. Dynamic buckling of elastic bars (the case of low velocity impact). Bull. JSME 15 (88), 1167–1175.

Hayashi, T., Sano, Y., 1972b. Dynamic buckling of elastic bars (the case of high velocity impact). Bull. JSME 15 (88), 1176–1184.

Jones, N., dos Reis, H.L.M., 1980. On the dynamic buckling of a simple elastic-plastic model. Int. J. of Solids and Structures 16, 969–989.

Jones, N., 1989. Recent studies on the dynamic plastic behavior of structures. Appl Mech Rev 42 (4), 95–115.

Jones, N., 1996. Recent studies on the dynamic plastic behavior of structures — an update. Appl Mech Rev 49 (10), S112–S117.

Karagiozova, D., Jones, N., 1992a. Dynamic buckling of a simple elastic-plastic model under pulse loading. Int. J. of Non-Linear Mechanics 27 (6), 981–1005.

Karagiozova, D., Jones, N., 1992b. Dynamic pulse buckling of a simple elastic-plastic model including axial inertia. Int. J. of Solid and Structures 29 (10), 1255–1272.

Karagiozova, D., Jones, N., 1995. Some observation on the dynamic elastic-plastic buckling of a structural model. Int. J. of Impact Engineering 16 (4), 621–635.

Karagiozova, D., Jones, N., 1996a. Multi-degrees of freedom model for dynamic buckling of an elastic-plastic structure. Int. J. of Solid and Structures 33 (23), 3377–3398.

Karagiozova, D., Jones, N., 1996b. Dynamic buckling of columns due to slamming loads. In: International Conference on Structures under shock and Impact, SUSI. Computational Mechanics Inc, Billerica, MA, USA, 311–320.

Lee, L.H.N., 1978. Quasi-bifurcation of rods with an axial plastic compressive wave. J. Appl. Mech 45, 100–104.

Lindberg, H.E., 1965. Impact buckling of a thin bar. J. Appl. Mech 32 (2), 315–322.

Lindberg, H.E., Florence, A.L., 1987. Dynamic Pulse Buckling — Theory and Experiment. Martinus Nijhoff, Dordrecht.

Nayfeh, A.H., 1973. Perturbation Method. Wiley, New York.

Simitses, G.J., 1987. Instability of dynamically-loaded structures. Appl. Mech. Rev 40 (10), 1403–1408.

Simitses, G.J., 1990. Dynamic Stability of Suddenly Loaded Structures. Springer-Verlag, New York.

Weller, T., Abramovich, H., Yaffe, R., 1989. Dynamic buckling of beams and plates subjected to axial impact. Computers and Structures 32 (3/4), 835–851.

Zhang, Q., Li, S., Zheng, J., 1992. Dynamic response, buckling and collapsing of elastic-plastic straight columns under axial solid-Fluid slamming compression. Part I: Experiments. Int. J. Solids and Structures 29 (3), 381–397.